ScienceAsia 29 (2003): **67-75**

Development of Mathematical Model for Continuous Spray Evaporator/Air (de)humidifier with Nonisothermal Polydisperse Droplets

Pratarn Wongsarivej and Wiwut Tanthapanichakoon*
Department of Chemical Engineering, Faculty of Engineering, Chulalongkorn University, Bangkok 10330, Thailand.
*Corresponding author, E-mail: fchwtt@eng.chula.ac.th

Received 30 Apr 2001
Accepted 13 Aug 2002

ABSTRACT A steady state model of co-current spray evaporator and air (de)humidifier for non-isothermal droplets has been developed to investigate the effect of polydispersity of droplet size on performance. The model is validated by comparison with results of Dickinson and Marshall (1968, AICHE J.14,541). It reveals that their ideal assumption of constant droplet temperature leads to significant error when the droplet size distribution is strongly polydisperse. Numerous simulation cases of the spray evaporator show that the average droplet diameter and droplet size distribution of water spray significantly affect the change in the air properties and the size, velocity and temperature of water droplets. For polydisperse droplets, a narrower droplet size distribution (σ=0.2) shows a more rapid decrease in the diameter of the droplets, thus causing a more rapid temperature decrease and humidity increase of the air than the case of a broader droplet size distribution (σ=0.4) with the same volume-averaged diameter.

KEYWORDS: evaporator, dehumidifier, polydisperse droplet, non-isothermal droplet.

INTRODUCTION

The evaporation/condensation of a volatile component (usually water vapor) from/on spray droplets involves simultaneous heat and mass transfer. Upon contact between atomized droplets and drying air, heat is transferred by convection from the air to the droplet, and converted to latent heat during moisture evaporation. The vaporized moisture is transported into the air by convection through the gas boundary layer that surrounds each droplet. The velocities of droplets leaving the nozzle of the atomizer may differ greatly from the velocity of the surrounding air, and simultaneously with heat and mass transfer, there is an exchange of momentum between the droplets and surroundings. The rate of heat and mass transfer is a function of temperature, humidity and transport properties of the air surrounding each droplet. It is also a function of the droplet diameter and relative velocity between the droplets and air.[1]

Humidification processes are carried out to control the humidity of an air space or, more usually, to cool and recycle process water through contact with low-humidity air. The directions of heat and mass transfer are determined by the relation between the humidity and temperature of the inlet gas phase and the temperature of the contacting liquid. The most obvious form of humidification equipment is the spray chamber. Here, the contacting liquid is sprayed as a mist into the gas stream. Gas velocity is kept low so that the contact time is high. Dehumidification processes are practised most commonly as a step in an air conditioning system. In this process, a warm vapor gas mixture is contacted with a cool liquid. Vapor condenses out of the gas phase, the gas phase cools, and the liquid is warmed. Both sensible and latent heat are transferred toward the liquid phase.[2]

Some notable contributors to spray evaporation analysis are Probert[3], Marshall[4], Shapiro and Erickson[5], Manning and Gauvin[6], Bose and Pei[7], Dickinson and Marshall[8], Keey and Pham[9], and Carslaw and Jaeger.[10] More specifically, Probert[3] presented a theoretical analysis based upon a spray size distribution following the Rosin-Rammler distribution. Polydisperse spray droplets were considered to have zero relative velocity with respect to the air stream and changes in the temperature driving force were assumed negligible during evaporation. Marshall[4] investigated spray evaporation of droplets following a logarithmic distribution, evaporating under zero relative velocity conditions and the same temperature driving force. Dickinson and Marshall[8] studied the spray evaporation under ideal conditions of constant droplet temperature and both negligible and significant relative velocity between the spray and air.

Since the rate of evaporation depends on the individual droplet size and the droplet temperatures are expected to vary during the first stage of water-air

contact, especially in the case of an evaporation tower, it was decided to develop a more rigorous mathematical model of the co-current spray evaporator, in order to investigate the effect of variable droplet temperature and polydispersity. In addition the spray droplets were considered to have variable relative velocity. In fact, the present model is readily applicable to the humidification and dehumidification processes.

Mathematical Model

The main assumptions of the model are as follows.

1. With the exception of the water droplets, the process is adiabatic and at steady state.

2. Air movement in the spray column may be approximated as plug flow with negligible heat conduction in the radial direction and negligible flow disturbance from the presence of the droplets.

3. Liquid droplets are essentially spherical and move vertically downwards. The effects of droplet coalescence, breakage and wall collision are negligible.

4. Droplets are uniformly distributed over the cross section of the vertical column. They are introduced into the spray chamber at the same arbitrary inlet velocity V_{po}.

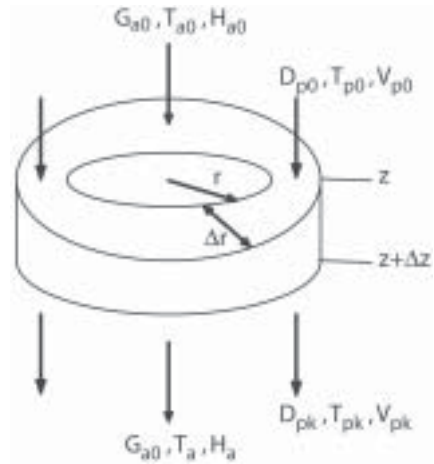

Fig 1. Control volume for heat and mass balances.

Case of Monodisperse Droplets

First we treat the case of monodisperse droplets of inlet diameter D_{po}. By considering simultaneous heat and mass transfer between the air and droplets within an annulus of differential thickness Δr and height Δz, as shown in Fig 1, five governing differential equations are derived as follows.[11]

Gas-phase water balance in the annulus:

(1)

Overall water balance in the annulus:

$$0 = 2\pi r\Delta r G_{a0} H\big|_{z=z} - 2\pi r\Delta r G_{a0} H\big|_{z=z+\Delta z} + \left(\frac{\pi D_p^3 \rho_p}{6}\right)(2\pi r\Delta r)\Big|_{z=z} - \left(\frac{\pi D_p^3 \rho_p}{6}\right)(2\pi r\Delta r)\Big|_{z=z+\Delta z} \tag{2}$$

Water-phase energy balance in the annulus:

$$0 = \frac{\pi D_p^3 \rho_p}{6}(2\pi r\Delta r C_p)(T_p - T_r)\Big|_{z=z} - \frac{\pi D_p^3 \rho_p}{6}(2\pi r\Delta r C_p)(T_p - T_r)\Big|_{z=z+\Delta z} + \pi 2\pi r\Delta r \frac{\Delta z}{V_p} h_c \pi D_p^2 (T_a - T_p) - \pi 2\pi r\Delta r \frac{\Delta z}{V_p} k_g \pi D_p^2 (H_p - H)\left[\lambda_p + C_v(T_a - T_p)\right] \tag{3}$$

Overall energy balance in the annulus:

$$0 = \frac{\pi D_p^3 \rho_p}{6}(2\pi r\Delta r C_p)(T_p - T_r)\Big|_{z=z} - \frac{\pi D_p^3 \rho_p}{6}(2\pi r\Delta r C_p)(T_p - T_r)\Big|_{z=z+\Delta z} + 2\pi r\Delta r G_{a0} C_h (T_a - T_r)\big|_{z=z} - 2\pi r\Delta r G_{a0} C_h (T_a - T_r)\big|_{z=z+\Delta z} + 2\pi r\Delta r G_{a0} \lambda_r H\big|_{z=z} - 2\pi r\Delta r G_{a0} \lambda_r H\big|_{z=z+\Delta z} \tag{4}$$

Equation of motion of one representative monodisperse droplet in the annulus:

$$\frac{\rho_p \pi D_p^3}{6}\frac{dV_p}{dt} = \frac{\rho_p \pi D_p^3}{6}\left(\frac{\rho_p - \rho_a}{\rho_p}\right)g - \left(\frac{\pi D_p^2 C_D \rho_a V_r}{8}\right)(V_p - V_a) \tag{5}$$

Divide equations (1) to (4) by $\Delta r\,\Delta z$, take $\lim_{\Delta z \to 0}$ and then rearrange the terms to obtain

$$\frac{dH}{dz} = \frac{\&h_c \pi D_p^2 (T_a - T_p)}{G_{a0}\lambda_p V_p} \tag{6}$$

$$\frac{dD_p}{dz} = \frac{-2h_c(T_a - T_p)}{\lambda_p V_p \rho_p} \tag{7}$$

$$\frac{dT_p}{dz} = \left(\frac{-6h_c}{\rho_p D_p V_p C_p}\right)\left[\begin{array}{l}\dfrac{\lambda_p(H_p - H)}{C_h} + \dfrac{C_v(H_p - H)(T_a - T_p)}{C_h} \\ -(T_a - T_p) - \dfrac{C_p(T_p - T_r)(T_a - T_p)}{\lambda_p}\end{array}\right] \tag{8}$$

$$\begin{aligned}\frac{dT_a}{dz} = {} & \left(\frac{\&h_c \pi D_p^2}{V_p G_{a0} C_h}\right)\left[\begin{array}{l}\dfrac{\lambda_p(H_p - H)}{C_h} + \dfrac{C_v(H_p - H)(T_a - T_p)}{C_h} \\ -(T_a - T_p) - \dfrac{C_p(T_p - T_r)(T_a - T_p)}{\lambda_p}\end{array}\right] \\ & + \left(\frac{\&h_c C_p \pi D_p^2}{V_p G_{a0} C_h \lambda_p}\right)(T_p - T_r)(T_a - T_p) \\ & - \left(\frac{\&h_c \pi D_p^2}{V_p G_{a0} C_h \lambda_p}\right)(T_a - T_p)\left[C_v(T_a - T_r) + \lambda_r\right]\end{aligned} \tag{9}$$

Since z is the position of the representative droplet, then $\frac{dz}{dt}$ is the droplet velocity, V_p. Multiplying the left hand side of equation (5) by $\frac{dz}{dt}$, after rearranging we obtain

$$\frac{dV_p}{dz} = \left(\frac{\rho_p - \rho_a}{\rho_p}\right)\frac{g}{V_p} - \left(\frac{3C_D \rho_a}{4D_p \rho_p V_p}\right)(V_p - V_a)^2 \tag{10}$$

where C_D is drag coefficient, C_h is heat capacity of humid air, C_p is heat capacity of water, C_v is heat capacity of water vapor, D is diameter, g is gravitational acceleration, G is mass velocity of air, h_c is convective film heat transfer coefficient, H is air humidity, H_p is saturated air humidity at droplet temperature, k_g is film mass transfer coefficient, n is the number-based droplet flux, r is the radial coordinate, T is temperature, V is velocity, z is the axial coordinate pointing downwards, λ is latent heat of vaporization and ρ is density. The meaning of the subscripts is as follows. 0 : inlet condition, a : air, p : water droplet and r : reference state.

Case of Polydisperse Droplets

It is assumed that the particle size distribution of the polydisperse droplets is given or known *a priori*. For simplicity, the inlet particles will be classified into ***kclss*** size fractions, say, ***kclss*** = 20 to 40. Each fraction is characterized by a single class size D_{pk}, which will change as a function of z as evaporation occurs. By considering all ***kclss*** class sizes and making a similar derivation as the monodisperse case, we obtain equations (11) to (15) in dimensionless forms as follows (k = 1, 2 , 3, … , ***kclss***) :

$$\frac{dH_a^*}{dz^*} = \pi\left(\frac{D_t}{D_{p0ave}}\right)\sum_{k=1}^{kclss}\left[\gamma_k^*\left(\frac{\&_k^* D_{pk}^{*2}}{V_{pk}^*}\right)\left(T_a^* - T_{pk}^*\right)\right] \tag{11}$$

$$\frac{dD_{pk}^*}{dz^*} = -2\left(\frac{D_t}{D_{p0ave}}\right)\left(\frac{h_{ck}\left(T_{a0}-T_{p0}\right)}{\rho_{pk}\lambda_{pk}V_{p0}}\right)\left(\frac{T_a^*-T_{pk}^*}{V_{pk}^*}\right) \tag{12}$$

$$\frac{dT_{pk}^*}{dz^*} = -6\left(\frac{D_t}{D_{p0ave}}\right)\left(\frac{h_{ck}}{\rho_{pk}C_{pp}V_{p0}}\right)\left(\frac{1}{D_{pk}^*V_{pk}^*}\right)$$
$$\left[\begin{array}{l}\beta_k^*\left(H_{pk}^*-H_a^*\right)+\left(\frac{C_v}{C_h}\right)\left(T_a^*-T_{pk}^*\right)\left(H_{pk}^*-H_a^*\right)\\ -\left(T_a^*-T_{pk}^*\right)-\alpha_k^*\left(T_a^*-T_{pk}^*\right)\left(T_{pk}^*-T_r^*\right)\end{array}\right] \tag{13}$$

$$\frac{dT_a^*}{dz^*} = \pi\left(\frac{D_t}{D_{p0ave}}\right)\sum_{k=1}^{kclss}\left\{\left[\begin{array}{l}\beta_k^*\left(H_{pk}^*-H_a^*\right)+\left(\frac{C_v}{C_h}\right)\left(T_a^*-T_{pk}^*\right)\left(H_{pk}^*-H_a^*\right)\\ -\left(T_a^*-T_{pk}^*\right)-\alpha_k^*\left(T_a^*-T_{pk}^*\right)\left(T_{pk}^*-T_r^*\right)\end{array}\right]\right.$$
$$\left.\left[\beta_k^*\gamma_k^*\left(\frac{\&_k^* D_{pk}^{*2}}{V_{pk}^*}\right)\right]\right\}$$
$$+\pi\left(\frac{D_t}{D_{p0ave}}\right)\sum_{k=1}^{kclss}\left[\gamma_k^*\left(\frac{C_{pp}}{C_h}\right)\left(\frac{\&_k^* D_{pk}^{*2}}{V_{pk}^*}\right)\left(T_a^*-T_{pk}^*\right)\left(T_{pk}^*-T_r^*\right)\right]$$
$$-\pi\left(\frac{D_t}{D_{p0ave}}\right)\left[\left(\frac{C_v}{C_h}\right)\left(T_a^*-T_r^*\right)+\frac{\lambda_r\left(T_{a0}-T_{p0}\right)}{C_h}\right]$$
$$\sum_{k=1}^{kclss}\left[\gamma_k^*\left(\frac{\&_k^* D_{pk}^{*2}}{V_{pj}^*}\right)\left(T_a^*-T_{pk}^*\right)\right] \tag{14}$$

$$\frac{dV_{pk}^*}{dz^*} = \left(\frac{\rho_{pk}-\rho_a}{\rho_{pk}}\right)\left(\frac{gD_t}{V_{p0}^2}\right)\left(\frac{1}{V_{pk}^*}\right)-\left(\frac{3C_D}{4}\right)\left(\frac{D_t}{D_{p0ave}}\right)\left(\frac{\rho_a}{\rho_{pk}}\right)\frac{(V_{pk}^*-V_{a0}^*)^2}{V_{pk}^*D_{pk}^*} \tag{15}$$

where[12]

$$h_{ck} = \frac{k_d}{D_{p0ave} D^*_{pk}} \left\{ 2.0 + 0.60 \sqrt{D^*_{pk} \left| V^*_{pk} - V^*_{a0} \right|} \left(\frac{C_{pa} \mu_a}{k_d} \right)^{0.33} \left(\frac{D_{p0ave} V_{p0} \rho_a}{\mu_a} \right)^{0.5} \right\} \quad (16)$$

k_d, C_{pa}, μ_a and are calculated at the film temperature, $T_f = \frac{(T_a + T_p)}{2}$

$$D_{p0ave} = \frac{\sum_{n=1}^{N} f_n(D_p)(D_p)}{100}, \quad D^*_{pk} = \frac{D_{pk}}{D_{p0ave}}, \quad H^*_a = H_a,$$

$$, \quad T^*_a = \left(\frac{T_a - T_{p0}}{T_{a0} - T_{p0}} \right),$$

$$T^*_{pk} = \left(\frac{T_{pk} - T_{p0}}{T_{a0} - T_{p0}} \right), \quad T^*_r = \left(\frac{T_r - T_{p0}}{T_{a0} - T_{p0}} \right), \quad V^*_{a0} = \frac{V_{a0}}{V_{p0}},$$

$$V^*_{pk} = \frac{V_{pk}}{V_{p0}}, \quad \Delta z^* = \frac{\Delta z}{D_t}, \quad \alpha^*_k = \frac{C_{pp}(T_{a0} - T_{p0})}{\lambda_{pk}},$$

$$H^*_{pk} = \frac{H_{pk} D^3_{p0ave}}{V_{p0}}, \quad \beta^*_k = \frac{\lambda_{pk}}{C_h (T_{a0} - T_{p0})}, \quad \gamma^*_k = \frac{h_{ck}(T_{a0} - T_{p0})}{\lambda_{pk} G_{a0}}, \quad k_d$$

is thermal conductivity, ***kclss*** is the total number of droplet class sizes, N is the total number of droplets and is viscosity. The meaning of the subscripts are as follows. ave : average, f : film, k : droplet class size number, and t : column. The superscript * means dimensionless value.

In the case of monodisperse droplets, we may use ***kclss*** =1. Equations (11) to (15) are integrated simultaneously using the fourth-order Runge-Kutta method. In the present model, the droplet temperature of each size fraction is not assumed to be constant, but varies with ***z***. In the case of polydisperse droplets, the droplet size distribution at the inlet will be represented by a sufficiently large number of droplet class sizes or fractions as shown in Table 1. The total number of ordinary differential equations is (3****kclss*** +2). The validation of the present model was carried out by comparing with the simulation results published by Dickinson and Marshall[8] (D-Mmodel) as shown in Fig 2. According to D-M model the definitions of the evaporation index, , on the horizontal axis and the unevaporated volume fraction on the vertical axis are given by

Table 1. Example of log-normal distribution (volume-averaged D_p=200 μm, σ=0.2) andinlet flux of droplets in each size fraction.

Fraction number (k)	Droplet class size (μm)	Representative diameter (μm)	Flux of droplets ($m^{-2}s^{-1}$)	Number of droplets (%)
1	0-40	20	4.67E-08	5.33E-13
2	40-80	60	8.75E+01	9.98E-04
3	80-120	100	1.10E+05	1.26E+00
4	120-160	140	1.75E+06	1.99E+01
5	160-200	180	3.61E+06	4.12E+01
6	200-240	220	2.33E+06	2.66E+01
7	240-280	260	7.62E+05	8.70E+00
8	280-320	300	1.67E+05	1.90E+00
9	320-360	340	2.87E+04	3.27E-01
10	360-400	380	4.29E+03	4.89E-02
11	400-440	420	5.92E+02	6.76E-03
12	440-480	460	7.85E+01	8.96E-04
13	480-520	500	1.02E+01	1.17E-04
14	520-560	540	1.34E+00	1.52E-05
15	560-600	580	1.76E-01	2.01E-06
16	600-640	620	2.37E-02	2.71E-07
17	640-680	660	3.27E-03	3.73E-08
18	680-720	700	4.62E-04	5.27E-09
19	720-760	740	6.73E-05	7.68E-10
20	760-800	780	1.01E-05	1.15E-10
			8.77E+06	1.00E+02

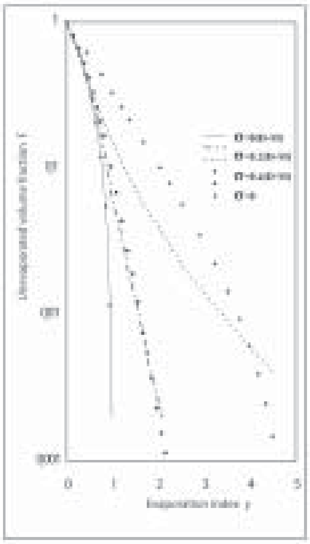

Fig 2. Comparison between the present model (dot) and Dickinson and Marshell (D-M) (lines) for log-normal polydisperse droplets.

$$y=\frac{\sum_{k=1}^{kclss}\left(D_{p0k}^2-D_{pk}^2\right)}{kclss}\ ,\quad F=\frac{\sum_{k=1}^{kclss}\left(\&_k D_{pk}^3\right)}{\sum_{k=1}^{kclss}\left(\&_k D_{p0k}^3\right)} \qquad (17)$$

The major difference between the two models is the assumption of constant droplet temperature in the D-M model. As expected, when the droplet size distribution is monodisperse (=0) or relatively narrow (=0.2, or ratio $=\frac{D_p atQ_r=85.13\%}{D_p atQ_r=15.87\%}=$ 1.49), the two simulation results agree well. Here, Q_r is the cumulative distribution. However, when the size distribution is strongly polydisperse (σ=0.4, or ratio = 2.26), the discrepancy may be attributed to the fact that the smaller droplets have much higher specific surface area and experience faster cooling effect than the larger ones. This means that the assumption of constant droplet temperature leads to significant error in the prediction when very small and large droplets coexist. In any case, the applicability of the present model has been confirmed.

Results and Discussion

Case of Monodisperse Droplets

To better understand the heat and mass transfer phenomena, we first consider the case of a monodisperse spray of water droplets. The conditions of simulation are as follows. The temperature, spray inlet velocity and mass velocity of droplets at the evaporator inlet are 333.16 K, 40.8 m s^{-1} and 0.036724 kg $m^{-2}s^{-1}$, respectively. The inlet air temperature, humidity and mass velocity are 533.16 K, 0.00 kg vapor kg^{-1}dry air and 0.5298 kg dry air $m^{-2}s^{-1}$, respectively. To clearly elucidate the phenomena, perfectly dry air is chosen. The suitable integration step size Δz has been found in advance to be 2×10^{-5} m. The three cases of monodisperse spray have inlet diameters of 50, 100 and 200 μm, respectively, with the same mass velocity.

Fig 3 reveals that when the droplets are smaller, the decreasing rate of droplet diameter is faster because small droplets have more surface area per volume than large ones. At steady state, the height required for complete evaporation of water droplets is only 0.1 m for D_{po} = 50 μm but increases to 1.2 m for D_{po} = 200 μm. Fig 4 confirms that the droplet temperature is not constant but shows a rapid decrease before increasing to a constant asymptotic value, which is essentially the wet-bulb temperature. Fig 5 shows a rapid drop in the droplet velocity near the inlet. As the droplet size decreases, the terminal velocity and the relative velocity of the droplets with respect to the air stream gradually

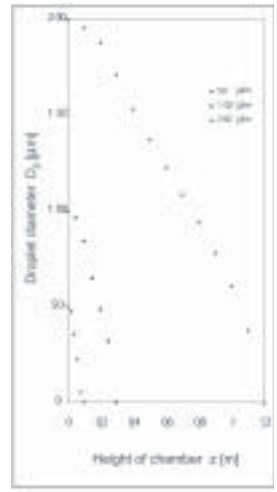

Fig 3. Relationship between droplet diameter and height of chamber for monodisperse droplets.

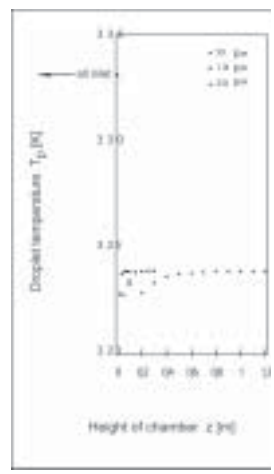

Fig 4. Relationship between droplet temperature and height of chamber for monodisperse droplets.

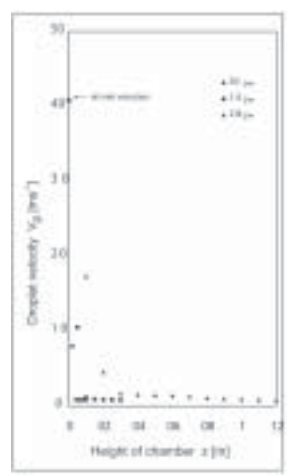

Fig 5. Relationship between droplet velocity and height of chamber for monodisperse droplets.

decrease. Similarly, Figs 6 and 7 show that a rapid decrease in the air temperature is accompanied by a corresponding increase in the air humidity. Smaller droplets effect a more rapid change in the air properties because they have greater surface area per volume than larger ones.

Case of Polydisperse Droplets

All simulation conditions are the same as the monodisperse case except the spray characteristics, which are as shown in Fig 8. The mathematical definition of log-normal distribution is

$$\frac{d(N)}{d(D)} = \frac{1}{D\sigma\sqrt{2\pi}} \exp\left[-\frac{\left(\ln D - \ln D_{GM}\right)^2}{2\sigma^2} \right] \qquad (18)$$

where $\boldsymbol{N}$ is the number of droplets of size between $\boldsymbol{D}$ and $\boldsymbol{D+dD}$, $\boldsymbol{D}$ is droplet diameter, $\sigma = \ln \sigma_G$ is the standard deviation, σ_G is the geometric standard deviation, and $\boldsymbol{D_{GM}}$ is the geometric mean diameter.[1] Note that, though the volume-averaged diameters for the two log-normal distributions in Fig 8 are the same, their inlet number-averaged diameters are 191.5 and 170.0 μm for $\sigma = 0.2$ and $\sigma = 0.4$, respectively. For simplicity, the entering droplets are divided into 20 class fractions.

Fig 9 shows that, in the case of polydisperse distributions, a size fraction with smaller droplets always evaporates faster than one with larger droplets. Since large droplets need longer distance to evaporate completely, the observed size distribution will no longer remain log-normal but change with the chamber height. Fig 10 shows that, as expected, smaller droplets show more rapid temperature change with the height than larger ones. Interestingly, the smallest droplets may experience notable sub-cooling in the early stage of evaporation, before all droplets reach essentially the same wet-bulb temperature. Fig 11 gives an example of the changes in droplet velocities with the chamber height for each size fraction of the droplets. As expected, the smaller the droplets, the lesser the distance it takes to reach the final terminal settling velocity. As evaporation occurs, the droplet size and its corresponding terminal velocity will become smaller. As a consequence, the distance required to reach the final velocity during evaporation will be longer than in the case of no evaporation. Fig 12 shows how th number-averaged $\boldsymbol{D_{pnum}}$ andvolume-averaged $\boldsymbol{D_{pvol}}$ droplet diameters change with the height. As expected, the narrower the droplet size distribution, the faster the change in average diameters. Therefore, the required height of the spray tower can significantly be reduced with the use of more nearly monodisperse spray. Though not shown here, it has been found that the narrower

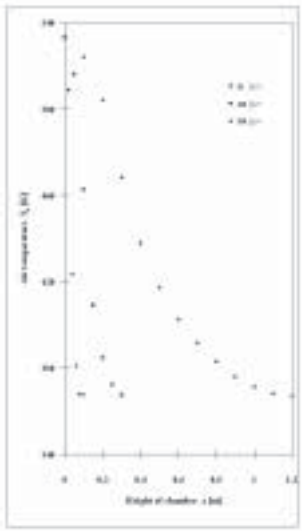

Fig 6. Relationship between air temperature and height of chamber for monodisperse droplets.

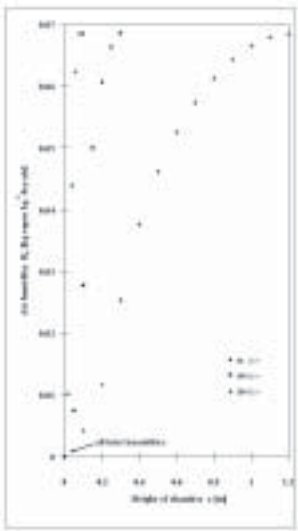

Fig 7. Relationship between air humidity and height of chamber for monodisperse droplets.

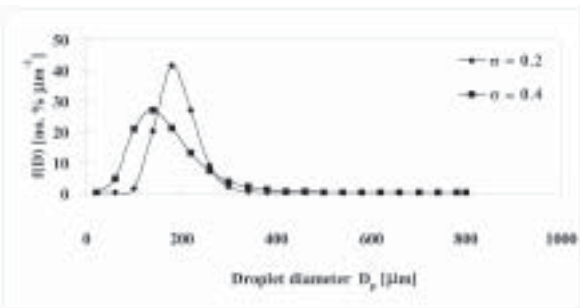

Fig 8. Log-normal inlet droplet size distribution (number basis)with the same volume-averaged diameter 200μm.

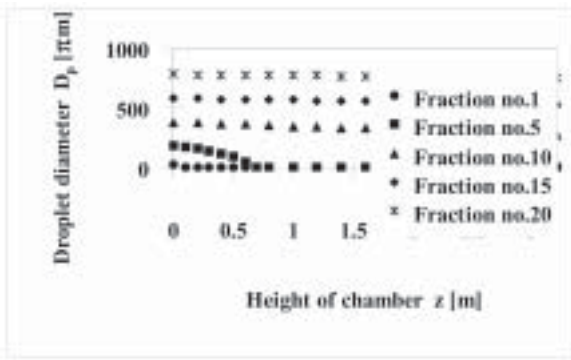

Fig 9. Relationship between droplet diameter and height of chamber for log-normal polydisperse droplets (σ=0.2).

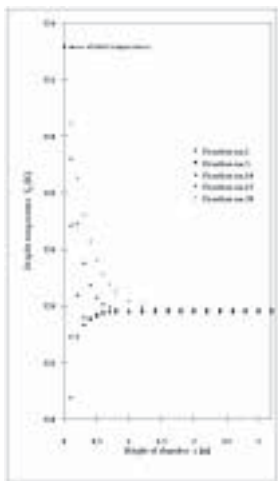

Fig 10. Relationship between droplet temperature and height of chamber for log-normal polydisperse droplets (σ=0.2).

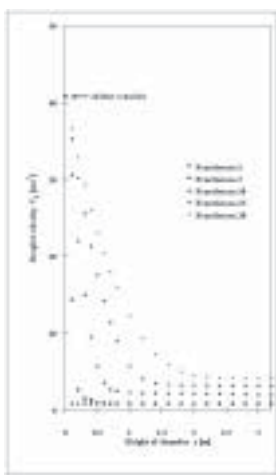

Fig 11. Relationship between droplet velocity and height of chamber for log-normal polydisperse droplets (σ=0.2).

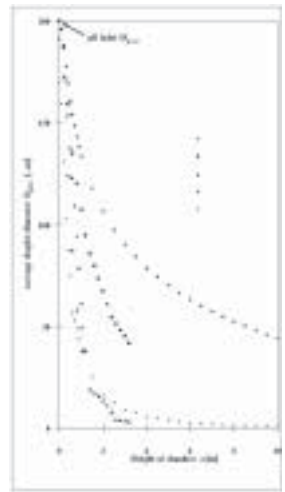

Fig 12. Effect of degree of polydispersity on the number- and volume-averaged droplet diameters.

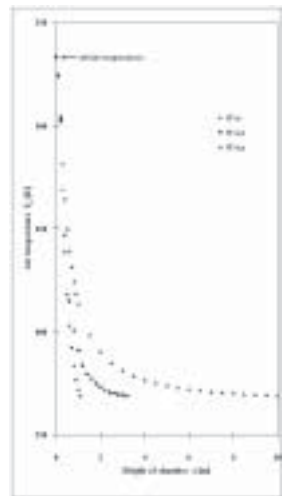

Fig 13. Effect of degree of polydispersity on the air temperture in the chamber.

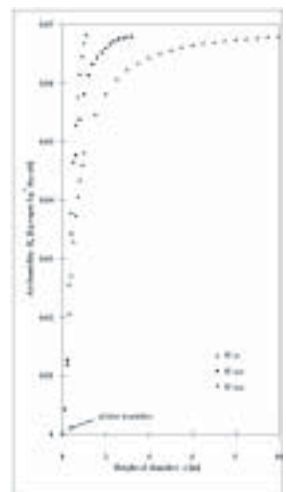

Fig 14. Effect of degree of polydispersity on the air humidity in the chamber.

droplet size distribution shows a slightly more rapid decrease in the average droplet temperature than the broader distribution. When σ =0.2, it takes up to 1 m for all the average temperatures to reach the wet-bulb temperature. Figs 13 and 14 show that, as expected from Fig 11, the narrower droplet size distribution results in a more rapid change in the air temperature and humidity than the broader distribution with the same volume-averaged diameter. Since the mass velocities of hot air and water spray are the same in all three cases, the final air temperatures and humidities become the same in all cases.

Conclusion

From Fig 12, the required effective height of an evaporator in the case of monodisperse spray can be as small as one-eighth of that with broad polydispersity (log-normal distribution with σ =0.4). Therefore, a manufacturer must pay great attention to the selection and performance of the atomizer. As for the generally accepted assumption of constant droplet temperature in the evaporator, Figs. 4 and 10 show that for an inlet volume-averaged droplet diameter of 200 μm, the droplets will not reach the wet-bulb temperature within the first 0.5 m, in the case of monodisperse droplets, and not within 1 m for the largest size fraction when σ = 0.2. Therefore, the said assumption could lead to significant error in the prediction.

Acknowledgements

WT received partial financial support from Senior Research Scholar Grant, 1998-2002, of the Thailand Research Fund.

References

1. Master K (1979) *Spray Drying Handbook*, 3rd ed, p 293. John Wiley & Sons, New York.
2. Foust AS (1980) *Principles of Unit Operations*, 2nd ed, p 437. John Wiley & Sons, New York.
3. Probert RP (1946) The influence of spray particle size and distribution in the combustion of oil droplets. *Phil Mag* **37**, 95.
4. Marshall WR (1955) Heat and mass transfer in spray drying. *Tran Amer Soc Mech Eng* **77** (11), 1377.
5. Shapiro AH and Erickson AJ (1957) Changing size spectrum of particle clouds undergoing evaporation, combustion, or acceleration. *J Amer Soc Mech Eng* **79**, 775.
6. Manning WP and Gauvin WH (1960) Heat and mass transfer to decelerating finely atomized sprays. *AIChE J* **6**, 184.
7. Bose AK and Pei DCT (1964) Evaporation rates in spray drying. *Can J Chem Eng* **42**, 259.
8. Dickinson DR and Marshall WR (1968) The rates of evaporation of sprays. *AIChE J* **14**, 541.
9. Keey RB and Pham Q (1977) Residence-time distribution of air in a tall-form spray chamber. *Chem Eng Sci* **32**, 1219.
10. Carslaw HS and Jaeger JC (1959) *Heat Conduction in Solids*. Oxford University Press.
11. Wongsarivej P (1997) Modelling of spray evaporation, humidifier/dehumidifier and cooling tower with co-current flow of air and water droplets. *M Eng Thesis*, Chulalongkorn University, Bangkok, Thailand.
12. Ranz WE and Marshall WR (1952) Evaporation from drops. *Chem Eng Prog* **48**, 141.